Available online at www.sciencedirect.com
SCIENCE DIRECT
Polymer 47 (2006) 341–345
polymer
www.elsevier.com/locate/polymer

Templating of crystallization and shear-induced self-assembly of single-wall carbon nanotubes in a polymer-nanocomposite

M.C. García-Gutiérrez [a,*], A. Nogales [a], D.R. Rueda [a], C. Domingo [a], J.V. García-Ramos [a], G. Broza [b], Z. Roslaniec [c], K. Schulte [b], R.J. Davies [d], T.A. Ezquerra [a,*]

[a] Department of Macromolecular Physics, Instituto de Estructura de la Materia, CSIC, Serrano 121, 28006 Madrid, Spain
[b] Technische Universität Hamburg-Harburg, Denickestrasse 15, D-21071 Hamburg, Germany
[c] Institute of Materials Science and Engineering, Szczecin University of Technology, Piastow Av. 19, PL-70310 Szczecin, Poland
[d] ESRF, B.P. 220, F-38043 Grenoble Cedex, France

Received 1 July 2005; received in revised form 11 October 2005; accepted 8 November 2005
Available online 28 November 2005

Abstract

We report the appearance of a novel self-assembling of a fraction of single-wall carbon nanotubes (SWCNT) within a SWCNT-polymer nanocomposite subjected to flow fields upon injection molding processing. By combining X-ray diffraction and Raman spectroscopy techniques, both working on a microfocus fashion, we probe that a fraction of the thinnest SWCNT self-assembles into a rectangular lattice in the sample regions where the shear stress induces the highest levels of nanotube aggregation. Additionally, we demonstrate that a modest amount in weight of nanotubes is enough to template the morphology of crystallization during flow providing a method to obtain a highly desirable fiber-like morphology.

Keywords: Templating of crystallization; Polymer-nanocomposite; SWCNT

1. Introduction

Single-wall carbon nanotubes (SWCNTs) exhibit a Young's modulus near the TeraPascal (TPa) range [1–3]. This makes them ideal as the reinforcing elements in a new generation of nanocomposite materials [1–3]. Such nanocomposites can be defined as nanofilled systems in which the total interfacial phase becomes the critical parameter, rather than the volume fraction of the filler [3]. The high aspect ratio and nanoscopic dimensions of carbon nanotubes (CNTs) give CNT-based nanocomposites specific properties differing from those achieved in classical composites [3,6]. A typical SWCNT sample consists of micron-size aggregates, frequently referred to as bundles or ropes, in which single nanotubes self-assemble in a two-dimensional hexagonal lattice [7–9]. Upon mixing with a polymeric matrix, nanometer-scale homogenization of the nanoparticles can be achieved by different methods [3,4,10–13].

In general, typical polymer and polymer-nanocomposite processing involves solidification from the molten state, either by crystallization or by vitrification. A consequence of such processing methods is the stresses induced by the combination of shear and elongational flow fields [14,16]. For example, polymer-nanocomposites have been studied by assessing the Raman spectra obtained from embedded SWCNTs subjected to strain and pressure [12,17]. Similarly, the effect of pressure on the structural distortion of SWCNT bundles has been revealed by X-ray scattering [8,9,17] and modeling has been reported [18]. However, the effect of flow fields similar to those used in industrial processing, both on the structure of a SWCNT within a nanocomposite and on the structure of the polymer matrix itself remain untreated until now. The influence of processing-induced flow fields on the nanostructure of polymer-nanocomposites is crucial because of the profound impact it has on physical properties [5,6,19].

In this paper, we report the effect of a combination of shear and elongational flow fields on the structure of nanoadditive and matrix for an injection molded SWCNT-polymer

* Corresponding authors. Tel.: +34 915616800; fax: +34 915645557.
E-mail addresses: imtc304@iem.cfmac.csic.es (M.C. García-Gutiérrez), imte155@iem.cfmac.csic.es (T.A. Ezquerra).

0032-3861/$ - see front matter © 2005 Elsevier Ltd. All rights reserved.
doi:10.1016/j.polymer.2005.11.018

nanocomposite. By combining microfocus X-ray diffraction and Raman spectroscopy techniques we observe that the flow field induces a novel self-assembling of SWCNT, not reported to date. Additionally, we demonstrate that a modest amount of SWCNTs is enough to template the crystalline morphology of the nanocomposite.

2. Experimental section

2.1. Materials and sample preparation

Nanocomposites of poly(butylene terephthalate) (PBT) ($M_w \approx 15{,}000$ g/mol) and oxidized single-wall carbon nanotubes (CNI Technology Co., Texas, USA, synthesized by using the HIPCO method) were prepared as previously described [20]. The nanocomposite was extruded from the reactor, pelletized and injection molded into long pieces with a rectangular cross section of 2×4 mm^2 (Fig. 1). The injection molding parameters were: injection pressure 25 bar, melt temperature 240–250 °C, mold temperature 40 °C, holding time 6 s and cooling time 20 s. The diameter of the SWCNTs, as characterized by Raman spectroscopy, ranges from about 0.6 to 1.4 nm. A SWCNT weight concentration of 0.2% was chosen because is the highest reachable by this method. As PBT is a semicrystalline polymer its use as a matrix in the nanocomposite allows the flow-field-induced structural changes to be identified.

2.2. Techniques

X-ray scattering measurements were performed at the European synchrotron radiation facility (ESRF) (Grenoble, France) microfocus beamline (ID13) using wavelength of 0.1 nm. The beamline was configured with crossed-mirror (KB) optics and collimator providing a 5 μm diameter beam with a guard aperture between the sample and collimator to reduce parasitic scattering [21]. It allows to record simultaneously WAXS and SAXS patterns when a sample-to-detector distance $D = 186.5$ mm is used. Data were recorded by a two dimensional MARCCD detector. The sample was scanned along a direction perpendicular to the injection flow (Fig. 1) in 50 μm steps. At every position a diffraction pattern was recorded in transmission. For background correction a pattern without sample contribution was recorded.

For Raman spectroscopy we used a Renishaw Microscope System RM2000 equipped with a Leica microscope, an electrically refrigerated CCD camera and a diode laser at 785 nm as exciting source. A beam size of 2 μm was used.

3. Results and discussion

3.1. Templating of crystallization

Fig. 1 shows X-ray scattering patterns from a PBT-SWCNT nanocomposite (top) and a pure PBT reference sample (bottom) prepared under identical conditions. The SAXS region of the pattern has been enlarged and presented separately. Patterns shown correspond to a position 0.8 mm from the sample edge. The patterns corresponding to pure PBT exhibit characteristic features of semicrystalline PBT [13]. The observed reflections from WAXS correspond to the α crystalline phase. The strong scattering concentrated around the beam center (SAXS region) corresponds to the long period related to the nanostructure typical of semicrystalline polymers [14]. Similar patterns were obtained with the sample rotated by 90°. The low degree of orientation, present only in some of the WAXS reflections [15], can be attributed to the moderate injection pressure used in sample preparation (2.5 MPa) as compared to those used in industrial processes (≈70 MPa) [16]. The situation is somewhat different for the nanocomposite sample (Fig. 1, top). In this instance, SAXS patterns reveal

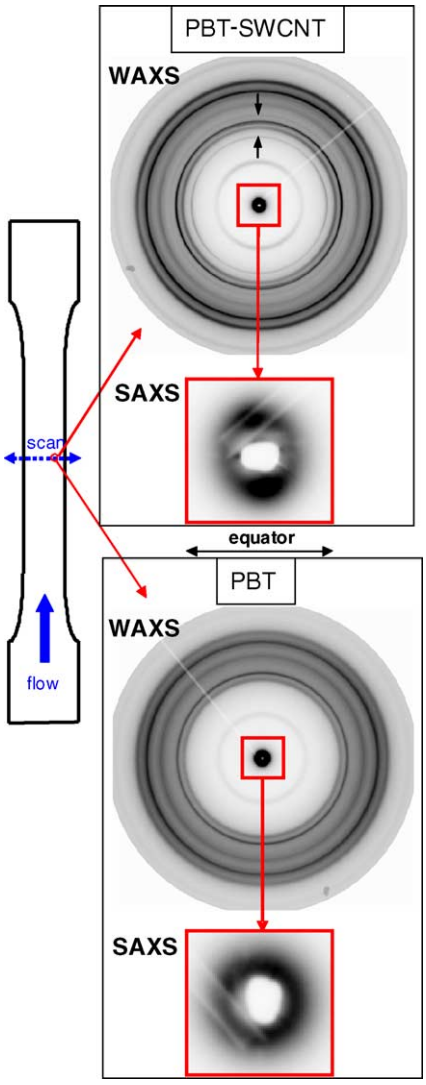

Fig. 1. Scheme of the injection molded sample (left). WAXS and SAXS patterns where taken along the dotted line in the middle of the sample in steps of 0.05 mm. X-ray patterns for both the poly(butylene terephthalate) (PBT) polymer and for the PBT-SWCNT nanocomposite with 0.2 wt% of SWCNT are shown in the lower and upper part, respectively. The SAXS angular region, closer to the center of the X-ray patterns, is shown magnified. The arrows drawn into the X-ray pattern of PBT-SWCNT indicate the presence of two extra reflections associated to a novel SWCNT self-assembly.

a clear orientation characterized by a concentration of the scattered intensity on the meridian. The orientation is not position dependent as identical SAXS patterns were recorded in a perpendicular direction. Considering that pure PBT reveals isotropic SAXS patterns then the orientation observed in the nanocomposite can be thought to be induced by the presence of SWCNT in the sample.

In a polymer, the chains in the melt extend in the direction of the flow field and tend to form extended threadlike precursors [22–25]. These precursors facilitate the epitaxial growth of folded chain lamellae filling the space perpendicular to the fibrillar precursor rendering to a characteristic oriented crystalline morphology [23]. The stability, after flow cessation, of the oriented morphology is a compromise between crystallization and chain relaxation [25]. In our case, for pure PBT the flow conditions are not enough to produce oriented morphology as derived from the SAXS ring patterns. However, for the nanocomposite, the existence of oriented crystallization morphology is evident as revealed by the oriented SAXS patterns.

To obtain oriented materials is a technological goal because of the significant improvements of their mechanical properties such as Young's modulus. In our case, an increment of about an 18% in the Young's modulus from 2.24 GPa for PBT to 2.65 GPa for the 0.2% nanocomposite has been measured from stress–strain experiments [26]. Of course, this improvement is not necessarily attributed solely to greater crystalline orientation, but may also be related to the inherent reinforcement properties of SWCNT. However, experiments performed on nanocomposite fibers made from SWCNT and poly(methyl methacrylate), which is an amorphous polymer, have shown no significant effect on the elastic modulus [27] even for 1% in weight of SWCNT. In addition, for the PBT-SWCNT nanocomposite, the presence of only 0.2% in weight of SWCNTs is enough to template the morphology of crystallization during flow.

3.2. Self-assembly of SWCNT

Even more striking is the information obtained from WAXS patterns (Fig. 1). As mentioned above, PBT exhibits the characteristic Bragg reflections of the α crystalline phase. In the nanocomposite, additionally to the structural features of the PBT matrix, there appear additional rings (two of them indicated by black arrows in Fig. 1) at q-values of ≈10 and 13 nm^{-1}, respectively. These reflections are position dependent as it is revealed by the sequence of diffractograms shown in Fig. 2 (top). Here, it can be seen that the extra reflections (indicated by the dashed lines) are detectable at positions starting from the edge until about 1 mm towards the center of the sample. One diffractrogram containing the extra reflections (signed by arrows) has been also presented in Fig. 2 (middle). In addition, we have included the diffractogram corresponding to the nanoadditive SWCNT (Fig. 2, bottom).

As mentioned before, native SWCNTs tend to organize themselves into bundles in which single nanotubes self-assemble in a two-dimensional hexagonal lattice exhibiting

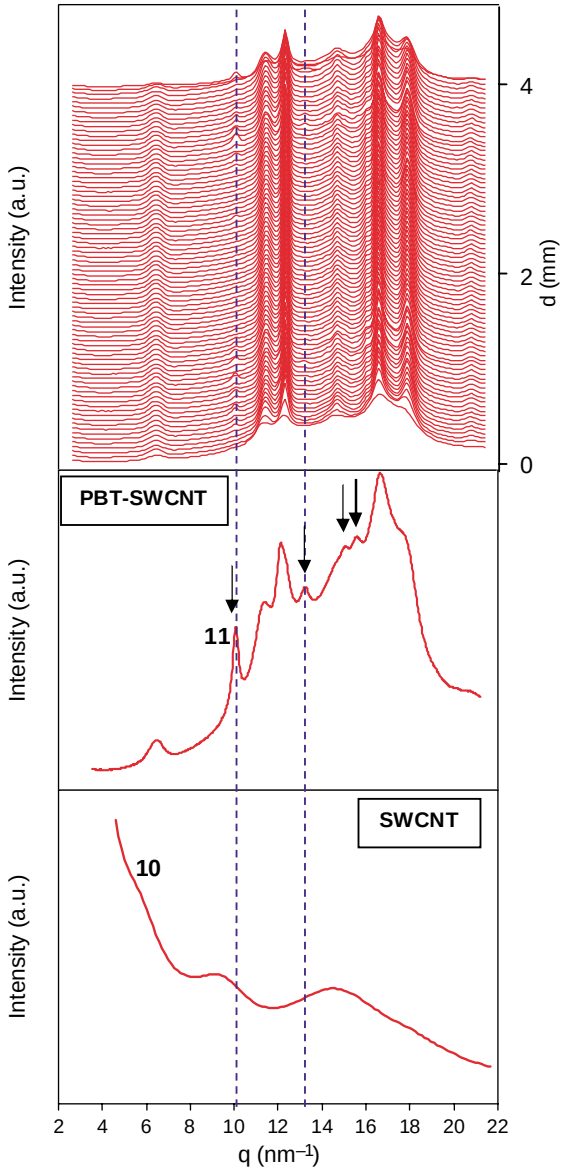

Fig. 2. Diffractograms from WAXS patterns of nanocomposite recorded as indicated in Fig. 1. Dotted lines indicate the position of the two extra reflections associated to a novel SWCNT self-assembly (top). WAXS diffractogram corresponding to the PBT-SWCNT at $d=0.05$ mm from the wall side of the sample. The arrows indicate the reflections associated to a novel SWCNT self-assembly (middle). WAXS diffractogram from native SWCNT used in the nanocomposite preparation (bottom).

the characteristic 10 reflection at $q \approx 4$–4.5 nm^{-1} along with several maxima at higher q-values corresponding to the different diffraction orders. In our case, the SWCNT sample exhibits this characteristic pattern (Fig. 2, bottom) in agreement with literature [8,9,17]. The 10 peak, appearing as a shoulder in the raw data, is affected by a strong continuous scattering due to the contribution of nanoparticles of different carboneous species and of nanovoids. The 10 reflection is absent in our WAXS patterns for the nanocomposite (Fig. 2, top) indicating a significant dispersion of the SWCNTs within the polymeric matrix. A deeper inspection of the diffraction patterns close to the edge (Fig. 2, middle) reveals that the two

extra reflections visualized in Fig. 1 (top) are accompanied by other two weak reflections which are absent in the PBT pattern. These four extra reflections can be indexed according to a rectangular centered two-dimensional crystal lattice with parameters: $a=0.94$ nm, $b=0.85$ nm. Since, there are two scattering objects in the unit cell the calculated molecular cross section is 0.3995 nm^2 what would define an object of 0.71 nm diameter.

A small fraction of SWCNTs of a similar diameter in size seems to be present in the nanoadditive according to the Raman spectrum of Fig. 3. Accordingly, it seems evident that, in the nanocomposite subjected to an elongational flow field, a fraction of the SWCNTs tends to self-assemble into a rectangular lattice which is not the expected hexagonal one for native SWCNTs. Considering that this unexpected packing of SWCNT appears in the regions close to the walls of the sample it seems plausible to attribute it to the shear stress which reaches a maximum in these regions and tends to zero in the center of the sample [16]. The question which immediately arises is: why only a fraction of the SWCNTs, that with smaller diameter, self-assembles. One possible explanation may come from the mechanical properties of SWCNTs. In particular, recent molecular dynamics simulations have shown that the collapse of SWCNTs is diameter dependent [18]. The collapse pressure of SWCNT increases linearly with increasing reciprocal diameter. We can hypothesize that, after the complete processing procedure, thinner SWCNT could be statistically longer and may, therefore, be more susceptible to alignment under the flow field than thicker ones. The maximum shear stress close to the wall may induce aggregation of the SWCNTs and a fraction of them, those of thinner diameter, may self-assemble into the rectangular lattice.

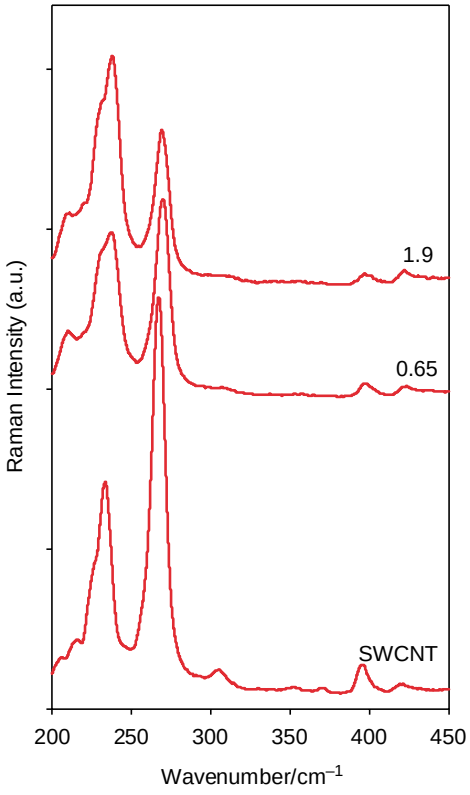

Fig. 3. Raman spectra in the region of the characteristic radial breathing modes (RBM) for pure SWCNT, and for the PBT-SWCNT nanocomposite at $d=$ 0.65 mm and $d=1.9$ mm from the wall side of the sample.

In order to further probe this hypothesis we performed Raman spectroscopy experiments in the spectral region covered by the characteristic radial breathing modes (RBM) of SWCNTs [12,17,28]. RBM appear due to vibrational modes of SWCNT and provide useful information about tube diameter but also about deformation [12] and aggregation [29]. In particular, it has been recently shown that the intensity of the band centered around 269 cm^{-1} can be used to probe nanotube aggregation. This characteristic band is almost absent for dispersed SWCNTs and increases, in relation to those appearing at lower frequency values, when the aggregation level increases [29]. Fig. 3 shows two selected Raman spectra, taken at different distances from the edge of the sample, in comparison with that of the pure SWCNTs, which exhibit a prominent band around 269 cm^{-1} indicating a high degree of aggregation [29]. In the nanocomposite, this band tends to decrease at expenses of those appearing at lower Raman frequency values, indicating a certain level of nanotube dispersion achieved in the nanocomposite preparation procedure [20]. It is clear that the band at 269 cm^{-1} from a spectrum taken closer to the sample center exhibits smaller intensity than that taken closer to the edge, indicating a higher level of nanotube aggregation closer to the sample wall.

Fig. 4 (top) shows the normalized area of the 237 cm^{-1} band in the nanocomposite as a function of the distance from the lateral sample surface. The dashed line indicates the level for SWCNT. Here, three regions can be differentiated. Firstly, close to the wall, $d<0.4$ mm, an increase of the area is observed indicating a decrease of the aggregation in relation to native SWCNT. In this region there is a characteristic skin effect induced by the metallic walls of the mold where the shear stress is disturbed by wall imperfections [30] and stresses that contribute to the intensity of the RBM and a shift in the position of the G' band [12]. Secondly, for $0.4<d$ (mm) <1 there is a stable zone in which the aggregation level is larger than in the previous region. This region can be associated with that where shear stress is more effective. Finally, for $d>1$ mm the aggregation level tends to decrease towards the center of the sample. In this region shear stress is expected to diminish towards the center of the sample and elongation flow becomes dominant. In the last two regions the G' band is constant at about 2570 cm^{-1} indicating no stresses and constrains on the SWCNT as in the first region [15]. As mentioned above, we propose that the self-assembly into a rectangular lattice of thinner SWCNT appear in the regions where the shear stress induces aggregation of the SWCNTs. Fig. 4 (bottom) shows the integrated intensity of the X-ray reflection identified as the 11 of a rectangular crystal lattice, as a function of the distance from the lateral sample surface. Here, the existence of the three regions can also be identified. Closer to the wall the intensity of the 11 reflection decreases parallel to the decrease in the aggregation level revealed by the Raman experiments.

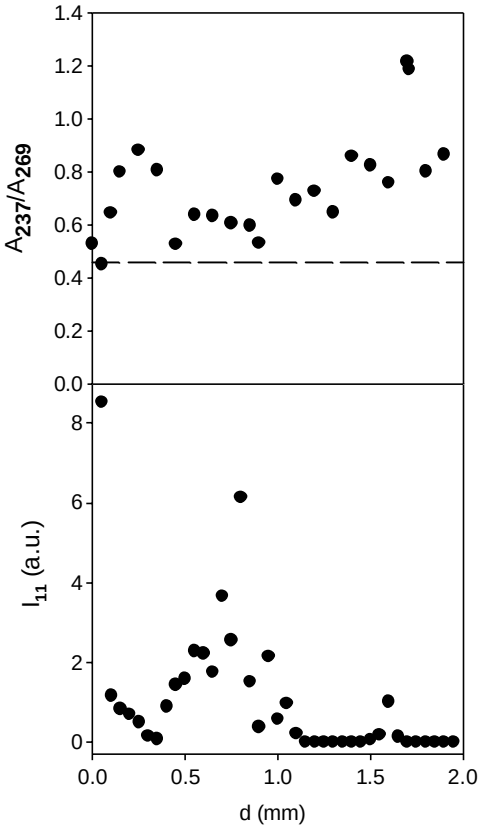

Fig. 4. Ratio of the Raman bands at 237 and 269 cm^{-1} as a function of the distance to the side wall of the sample. The dashed line represents the value for pure SWCNT (top). Integrated intensity of the 11 reflection of the novel assembly of SWCNT identified as a rectangular crystal lattice (bottom).

In the intermediate zone, where aggregation according to the Raman measurements is higher, the intensity of the reflection reaches its maximum. Finally, in the third region the intensity vanishes coinciding with the increment of the nanotube dispersion towards the center of the sample.

4. Conclusions

In conclusion, we have demonstrated that flow fields, mimicking those used in industrial processing, have a strong impact on the bundle structure of SWCNT within a nanocomposite and on the structure of the polymer matrix. A combination of X-ray and Raman spectroscopy, both working on microfocus fashion, have proven that shear stresses tend to self-assemble the nanotubes into a novel lattice, different from that of native SWCNTs. Additionally, we have shown that the presence of only 0.2% in weight of SWCNTs is enough to template the morphology of crystallization during flow, providing a method to obtain a highly desirable fiber-like morphology.

Acknowledgements

The diffractogram of native SWCNTs has been collected at BM16 (ESRF) with the help of A. Labrador, D. Beltrán and E. Fraga. This investigation has been performed under the auspices of the CNT-NET (GTC1-2000-28052), the MERG-CT-2004-505674 and the MERG-CT-2004-511908 from the UE. The authors thank the financial support from the MCYT (grant FPA2001-2139), Spain. M.C.G.G. is also grateful to the Comunidad Autónoma de Madrid for the support of this research.

References

[1] Treacy MMJ, Ebbesen TW, Gibson JM. Nature (London) 1996;381:678.
[2] Lourie O, Cox DM, Wagner HD. Phys Rev Lett 1998;81:1638.
[3] Vaia RA, Wagner HD. Mater Today 2004;32.
[4] Sandler JKW, Kirk JE, Kinloch IA, Shaffer MSP, Windle AH. Polymer 2003;44:5893.
[5] Gorriasi G. Polymer 2003;44:2271.
[6] Vaia RA. Adv Mater 1995;7:154.
[7] Thess A, Lee R, Nikolaev P, Dai HJ, Petit P, Robert J et al. Science 1996; 273:483.
[8] Rols S, Righi A, Alvarez L, Anglaret E, Almairac R, Journet C et al. Eur Phys J B 2000;18:201.
[9] Rols S, Goncharenko IN, Almairac R, Sauvajol JL, Mirebeau I. Phys Rev B 2001;64:153401.
[10] Pötschke P, Dudkin SM, Alig I. Polymer 2003; 44:5023.
[11] Barrau S, Demont P, Peigney A, Laurent C, Lacabanne C. Macromolecules 2003;36:5187.
[12] Lucas M, Young RJ. Phys Rev B 2004;69:085405.
[13] Nogales A, Broza G, Roslaniec A, Schulte K, Sics I, Hsiao BS et al. Macromolecules 2004;37:7669.
[14] Peterlin A. Colloid Polym Sci 1987;265:357.
[15] García-Gutiérrez MC, Nogales A, Rueda DR, Domingo C, García-Ramos JV, Broza G et al. Submitted for publication.
[16] Kumaraswamy G, Verma RK, Kornfield JA. Rev Sci Instrum 1999;70: 2097.
[17] Karmatar S, Sharma SM, Teredasai PV. New J Phys 2003;5:1431.
[18] Elliott JA, Sandler JKW, Windle AH, Young RJ, Shaffer MSP. Phys Rev Lett 2004;9:955011.
[19] Gao F. Mater Today 2004;50.
[20] Roslaniec Z, Broza G, Schulte K. Compos Interfaces 2003;10:95.
[21] Riekel C. Rep Prog Phys 2000;63:233.
[22] Keller A, Kolnaar HWH. Mater Sci Technol 1997;18:189.
[23] Somani R, Hsiao BS, Nogales A, Srinivas S, Tsou AH, Sics I et al. Macromolecules 2000;33:9385.
[24] Kumaraswamy G, Issaian AM, Kornfield JA. Macromolecules 1999;32: 7537.
[25] García Gutiérrez MC, Alfonso GC, Riekel C, Azzurri F. Macromolecules 2004;37:478.
[26] Broza G, Kwiatkowska M, Roslaniec Z, Schulte K. Polymer; 2005;46: 5860.
[27] Haggenmueller R, Gommans HH, Rinzler AG, Fischer JE, Winey KI. Chem Phys Lett 2000;330:219.
[28] Bandow S, Asaka S, Saito Y, Rao AM, Grigorian L, Richter E. Phys Rev Lett 1998;80:3779.
[29] Heller DA, Barone PW, Swanson JP, Mayhofer RM, Strano MS. J Phys Chem B 2004;108:6905.
[30] Gray GW, Winsor PA. Liquid crystals and ordered fluids. New York: Plenum Press; 1985.